NPS67-85-012CR

# NAVAL POSTGRADUATE SCHOOL

## Monterey, California

CONTRACTOR REPORT

# MEASUREMENTS AND DESIGNS RELATED TO ELECTRICAL SPRAY MODIFICATION IN A T-56 COMBUSTOR

by

Zeev Shavit

December 1985



Prepared for:
Naval Postgraduate School
y, California 93943

NAVAL POSTGRADUATE SCHOOL
Monterey, California

RADM R. H. Shumaker
Superintendent

D. A. Schrady
Provost

The work reported herein was carried out for the Naval Postgraduate School by Mr. Zeev Shavit under Contract Number N62271-84-M-3039. The work presented in in this report is part of a project sponsored by NAVAIR on Advanced Aircraft Propulsion Systems and is under the cognizance of Professor O. Biblarz and J. A. Miller.



This report was prepared by:

UNCLASSIFIED

SECURITY CLASSIFICATION OF THIS PAGE (When Data Entered)

## REPORT DOCUMENTATION PAGE

READ INSTRUCTIONS BEFORE COMPLETING FORM

| | |
|---|---|
| 1. REPORT NUMBER: NPS67-85-012CR | 2. GOVT ACCESSION NO. |
| 3. RECIPIENT'S CATALOG NUMBER | |
| 4. TITLE (and Subtitle): Measurements and Designs Related to Electrical Spray Modification in a T-56 Combustor | 5. TYPE OF REPORT & PERIOD COVERED: Contractor Report, August 84 - September 85 |
| 6. PERFORMING ORG. REPORT NUMBER | |
| 7. AUTHOR(s): Zeev Shavit | 8. CONTRACT OR GRANT NUMBER(s): N62271-84-M-3039 |
| 9. PERFORMING ORGANIZATION NAME AND ADDRESS: Naval Postgraduate School, Monterey, California 93943 | 10. PROGRAM ELEMENT, PROJECT, TASK AREA & WORK UNIT NUMBERS |
| 11. CONTROLLING OFFICE NAME AND ADDRESS: Mr. George Derderian, Naval Air Systems Command, Washington, D.C. 20631 | 12. REPORT DATE: December 1985 |
| | 13. NUMBER OF PAGES: 54 |
| 14. MONITORING AGENCY NAME & ADDRESS(if different from Controlling Office): Naval Postgraduate School, Monterey, California 93943 | 15. SECURITY CLASS. (of this report): Unclassified |
| | 15a. DECLASSIFICATION/DOWNGRADING SCHEDULE |

16. DISTRIBUTION STATEMENT (of this Report)

Approved for public release; distribution unlimited

17. DISTRIBUTION STATEMENT (of the abstract entered in Block 20, if different from Report)

18. SUPPLEMENTARY NOTES

19. KEY WORDS (Continue on reverse side if necessary and identify by block number)

Particle measurment, Sauter Mean Diameter, T56 combustor, electrostatic atomization, alternative fuels

20. ABSTRACT (Continue on reverse side if necessary and identify by block number)

(SEE REVERSE SIDE)



DD FORM 1 JAN 73 1473 EDITION OF 1 NOV 65 IS OBSOLETE

S/N 0102-LF-014-6601

UNCLASSIFIED

SECURITY CLASSIFICATION OF THIS PAGE (When Data Entered)

## ABSTRACT

A new optical technique for measuring Sauter Mean Diameter changes of a fuel spray under an electrostsatic field was checked, calibrated, and implemented. The optical technique is based on measuring scattered light at two angles using a variable focal length apparatus. Special attention was given to improving the electrical control loop parameters in order to minimize measurement errors.

In order to measure more realistically the effects of the electrostatic probe inside a gas turbine combustor, a pressure chamber was added to the outlet of the present combustion simulation device. Hot tests were carried out with diesel (DF-2) fuel. Pressure chamber, combustor's temperatures, fuel, and air mass flow rates, were recorded together with the voltage applied at the electrode.

Results of the cold tests with the new optical device show a Sauter Mean Diameter of 50.0 micron at fuel presuure (DF-2) of 100 psi, 51.7 micron at 125 psi and 47.8 micron at 80 psi. The device could not resolve changes while the high voltage field was exerted. Combustion temperatures with the pressure chamber are presented. Preliminary designs for improvements of the various devices are also described here.

ABSTRACT

A new optical technique for measuring Sauter Mean Diameter changes of a fuel spray under an electrostsatic field was checked, calibrated, and implemented. The optical technique is based on measuring scattered light at two angles using a variable focal length apparatus. Special attention was given to improving the electrical control loop parameters in order to minimize measurement errors.

In order to measure more realistically the effects of the electrostatic probe inside a gas turbine combustor, a pressure chamber was added to the outlet of the present combustion simulation device. Hot tests were carried out with diesel (DF-2) fuel. Pressure chamber, combustor's temperatures, fuel, and air mass flow rates, were recorded together with the voltage applied at the electrode.

Results of the cold tests with the new optical device show a Sauter Mean Diameter of 50.0 micron at fuel presuure (DF-2) of 100 psi, 51.7 micron at 125 psi and 47.8 micron at 80 psi. The device could not resolve changes while the high voltage field was exerted. Combustion temperatures with the pressure chamber are presented. Preliminary designs for improvements of the various devices are also described here.

ACKNOWLEDGEMENTS

The author wishes to express his gratitude to Professor Oscar Biblarz and Professor James Miller for providing the opportunity to perform this work during his sabbatical, and for their support in participation as well as for the many valuable discussions. To the support of the technical staff of the Aeronautics department: to Bob Besel, Ted Dunton, Glenn Middleton, Mike Odell, Pat Hickey and Don Harvey, also may thanks.

TABLE OF CONTENTS

1. INTRODUCTION.....6

2. COLD TESTS.....7

2.1 ANALYSIS.....7

2.2 DESCRIPTION OF INSTRUMENT.....14

2.3 CALIBRATION AND OPERATION.....19

2.4 MEASUREMENTS.....22

2.5 CONCLUSIONS FOR THE COLD TESTS.....23

3. PROPOSED IMROVEMENTS FOR THE OPTICAL DEVICE.....23

4. CHANGING POLES IN THE HIGH VOLTAGE FUEL NOZZLE.....30

5. HOT TESTS.....35

5.1 PREPARATIONS.....35

5.2 HOT TESTS MEASUREMENTS.....42

5.3 HOT TESTS IMPROVEMENTS.....46

6. CONCLUSIONS.....50

LIST OF FIGURES

1.BASIC OPTICAL SYSTEM FOR FORWARD SCATTERED LIGHT.....8

2. TWO ANGLE MEASUREMENT.....11

3.ERROR RATIO OF METHOD 1, $\lambda$ = 0.6328 micron.....13

4. COMPARTION BETWEEN THEORY AND MEASUREMENTS, VARIABLE FOCAL LENGTH CONTROL WITH VARIOUS INTENSITY RATIOS .....15

5. SCHEMATIC DIAGRAM OF OPTICAL EXPERIMENT APPARATUS.....16

6. OPPTICAL APPARATUS- WITHOUT TUBE COVER.....17

7. OPTICAL APPARATUS- WITH TUBE COVER.....18

8. NORMALIZED RESOLUTION AS A FUNCTION OF INTENSITY RATIO.....21

9. OBJECTIVE MOVABLE HOLDER AND DEVICE LEANING LEGS.....25

10. OPTIC DEVICE CROSS SECTION.....27

11. SPRAY NOZZLE HEAD INSULATION.....32

12. FLY- SWATER AND TEFLON CAP IN COLD TEST ARRANGEMENT..33

13. PRESSURE CHAMBER NOZZLE.....37

14. PRESSURE CHAMBER.....38

15. COMBUSTION AND PRESSURE CHAMBERS.....40

16. SCHEMATIC DIAGRAM OF THE COMBUSTION APPARATUS.....41

17. TEMPERATURE- VOLTAGE DISTRIBUTION WITH TIME.....44

18. INSULATING THE FUEL SPRRAY NOZZLE MOUNTING.....47

19. MULTI-PURPOSE PROBE - PRELIMINARY DESIGN.....48

# LIST OF TABLES

1 HOT TEST RESULTS.....45

# 1. INTRODUCTION

The work presented here is part of a research program on the subject of improving fuel burning. The fuel burns in a jet engine combustor can with the aid of high-voltage-electric field spraying.

The work was divided into three main parts. The first part consisted of cold tests in which, with the aid of a special optical device developed and described in Ref.1, we tried to determine changes in fuel droplet size as the drops emerged from a fuel spray. The second part of that work was to design high voltage connections and a presure chamber for the T-56 jet combustor. The last part of this research was to measure the preformance in the aboved mentioned combustor with the pressure chamber incorporated.

The cold test portion of this work concentrated in calibrating and finding the measurement error of the radiometer in order to get a better resolution, and to be able to ditinquish changes in the particle size resulting from an electric field in the fuel spray zone. Previous measurements, done by A. Zajdman ( Ref. 2), were based on the change of the total intensity attenuation of a lobe of light crossing a spray with and without the high voltage field. The high voltage field causes repulsion of the droplets together with a change of size, (Ref. 11). The combination of these two parameters affects the intensity attenuation of a ray light moving through the spray. Because of cone angle changes, spray cone angle must be measured simultaneously. After carrying out a literature survey, an improved method for measuring the Sauter Mean Diameter (SMD) in the cross section of light and spray was proposed (Ref. 1). A prototype optical

device based on a variable focal length radiometer was built, calibrated against standard particles, and then used to measure the SMD in the fuel spray.

In order to find the effects of the high voltage field on the combustion efficiency, it was a necessary to operate the combustor under higher pressure than atmospheric. A pressure chamber and two different size exit nozzles, for two different flow rate regions, were designed and manufactured. Testing with the complete device showed that the pressure head added by the nozzle caused a drop of the flow rate of air supplied by the compressor resulting in a maximum combustor pressure of 2 atm. Tests were conducted with diesel fuel; temperatures, fuel and air rate flow, pressure and voltage were recorded.

## 2. COLD TESTS.

The idea of measuring the change in the SMD under an high voltage field (Ref. 3), lead us to build an optical device with minimum resolusion error. The basic theory, upon which the device is based, the main principles of work and how it was applied to the droplet measurements will be shown in this section.

### 2.1 Analysis

When a collimated beam of light passes through an aerosol cloud, it is scattered by the aerosol particles at an angle which is proportional to the size of the particle. If this beam is subsequently focused by an objective lens, as shown in Fig. 1, one finds that the beam cannot be focused on a single point, as would be

possible in the absence of scattering.

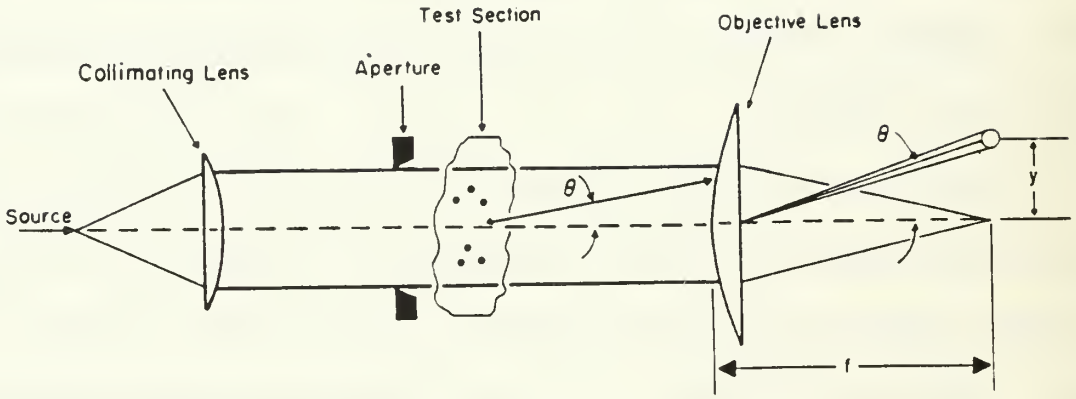


Figure 1. BASIC OPTICAL SYSTEM FOR FORWARD SCATTERED LIGHT

The intensity distribution of the light in the focal plane is found to be a function of three parameters: The focal-length of the device, the wavelength of the light source, and the size distribution of the particles in the aerosol. These parameters may be represented as two dimensionless quantities. The particle size and wavelength may be combined to a normalized parameter, called $\alpha_{32}$ , defined as:

$$(1)\ \alpha_{32} = \pi D_{32}/\lambda$$

where $D_{32}$ and $\lambda$ are the Sauter Mean Diameter and the wavelength of the light source respectively. The second quantity is the deflection angle, $\theta$, which for in small scattering angles may be written as:

$$(2)\ \theta = Y/f$$

Where y is the distance from the center in the focal plane and f is objective focal-length.

When particles in the aerosol cloud have a single diameter, Fraunhofer theory shows that for such monodispersion, the forward scattered light intensity at each point y divided by the intensity at the center, is a function of $\alpha_{32}$ and $\theta$ :

$$(3)\ I(\theta)/I(0) = [2J_1(\alpha \mathrm{Sin}\theta) / (\alpha \mathrm{Sin}\theta)]^2$$

Where I(0) is the intensity in the center $\theta$ =0 and $J_1$ is a first order Bessel function of the first kind. The intensity profile of a polydispersed aerosol may be represented (9) by an integral of equation 3 over the range of particle sizes modified by the concentration profile. The concentration may be taken into account by a weighting function $n(\alpha)$, and the integral has the form of:

$$(4)\quad I(\theta) = \int n(\alpha)[2J_1(\alpha \mathrm{Sin}\theta) / \alpha\theta]^2 d\alpha$$

Dobbins (4) has shown that the intensity ratio given by Eq.4 may be approximated by a Gaussian distribution function within 5 percent for values of $\alpha\theta$ less than 3. Ruscello (10) has shown that a good approximation for aerosol droplets having a Sauter Mean Diameter of 60 microns is obtained when a Gaussian distribution is assumed as long as a mean standard deviation of at least 10 microns is present in the aerosol.

The Fraunhofer intensity ratio in which the integral expression is replaced with a Gaussian distribution becomes a relatively simple exponential function of the two dimensionless parameters $\alpha$ and $\theta$:

$$(5)\quad I(\theta)/I(0) = \exp[-(0.57\,\alpha_{32}\theta)^2]$$

In order to minimize sensitivity errors it is desireable to locate the two photodetectors on opposite sides of the inflection point in the distribution function, located at $\alpha\theta$ =1.24, as shown in Fig. 2, corresponding an intensity ratio $I(\theta)/I(0)$=0.606.

The intensity ratio $I_2/I_1$ corresponding to two locations of the photodetector, $\theta_1$, and $\theta_2$ ,may be obtained from Eq.5:

$$(6)\quad I_2/I_1 = \exp[-(o.57\,\alpha_{32})^2(\theta_2^2 - \theta_1^2)]$$

Using the definitions of $\alpha_{32}$ and $\theta$, Eqs. 1 and 2, we may obtain from Eq. 6 an expression for $D_{32}$ , the Sauter Mean Diameter:

$$(7)\quad D_{32} = (\lambda/0.57\pi)(f/y_1)\sqrt{\ell n(-I_2/I_1)/[(Y_2/Y_1)^2-1]}$$

Two measurement techniques based on Eq.7 suggest themselves. Both use a fixed focal-length device, as shown in Fig. 1. The first method employs two fixed photodetector locations ($y_1$ and $y_1$ constant) and the intensities $I_1$ and $I_2$ are measured. With knowledge of $y_1$, f, $y\sigma'^2O$ and $\lambda$, theintensities $I_1$ and $I_2$ give a direct expression for $D_{32}$ (Eq.7). In the second technique, a single photodetector location is swept through the focal plane until a constant intensity ratio point is reached. In this case $y_2$ is to be measured while $I_2/I_1$, f and $y_1$ are known.

An uncertainty analysis made by Buchele (8) shows that for $\lambda$ =0.6328 micron and $\theta_1$ = 0.003 radians the first technique is limited to the measurement of Sauter Mean Diameters greater than 100 microns. In both techniques the location of the one of the photodetectors determines the largest particle diameter, while the accuracy of the measurement of $Y_2/Y_1$ in the first technique and of $I_2/I_1$ in the second technique determines the uncertainty in $D_{32}$For example Buchele (8) has shown that of $\theta_1$ = 0.003 radians, the uncertainty is less than 4 percent in each of the two techniques for the following combination of parameters:

Technique 1:

| Largest SMD (microns) | $y_2/y_1$ |
|---|---|
| 70 | 3 |
| 100 | 2 |
| 120 | 1.5 |

Technique 2: the largest particle diameter will be 110 micron for $I_2/I_1$ equal to 0.5. Shown in Fig. 3 is the effect of $\theta_1$ on Sauter Mean Diameter range for fixed uncertainty.

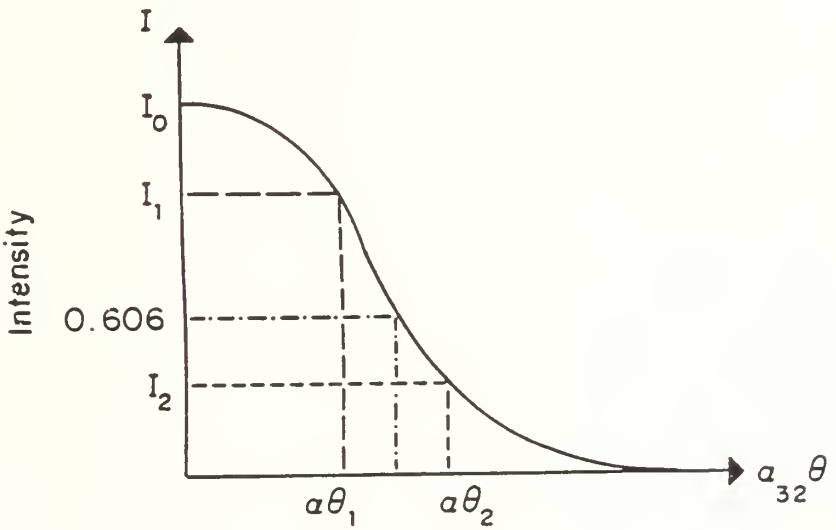


Figure 2. Two angle measurement.
(from ref. 8)

In order to improve the the flexibility of the two standard techniques described aboved, if it was decided to introduce an objective of variable focal-length, f. This produces an optical effect which is equivalent to changing $\theta_1$ while the off axis distance, $y_1$, remains constant. Thus for fixed $y_1$ and $y_2$ the ratio $\theta_1/\theta_2$ may be held constant while any value of $\theta_1$ may be selected,(within the range of objective focal-length available). In this way optimal sensitivity may be maintained over a wide range of aerosol particle diameters as is seen in Fig. 3. A second advantage is that an optimal intensity ratio may be obtained with fixed photodetector locations, or conversly a focal length corresponding to a fixed intensity ratio may be obtained for a given aerosol, corresponding to its Sauter Mean Diameter.

In practice a portion of the optical path has been replaced by a photographic zoom lens whose focal length is controlled by a servo mechanism under control of the signals derived from the output of the two photodetectors, i.e. $I_1$ and $I_2$ The ratio $I_2/I_1$ may be set by the operator as a control parameter. The expanded ability to detect various sized aerosols is shown in Fig. 4 where one sees also that the range is only limited by the span of the focal-lengths available.

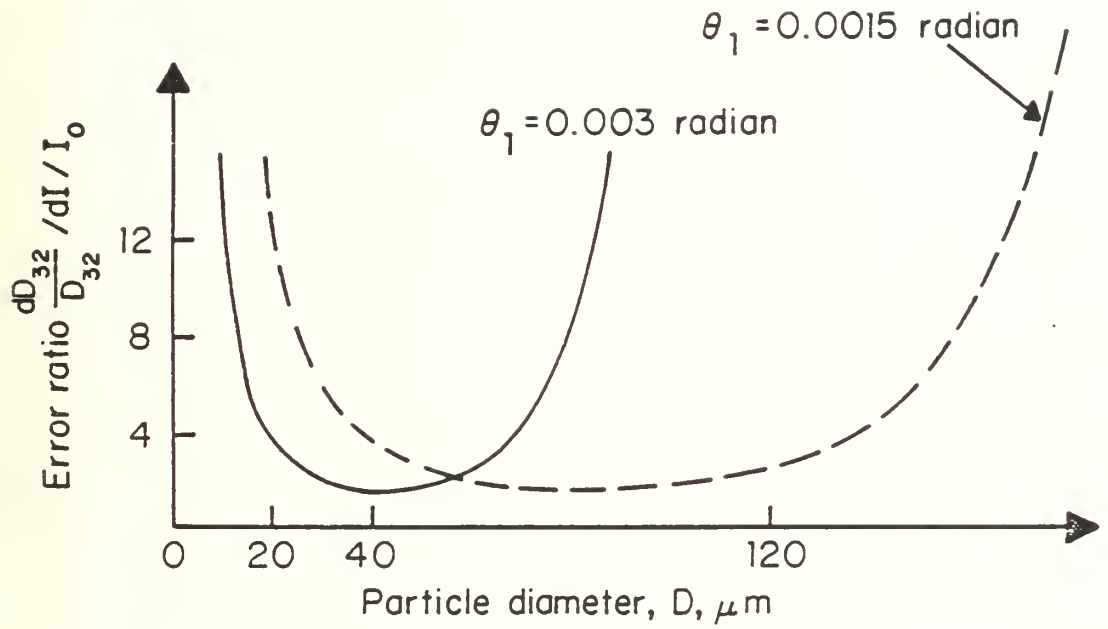


Figure 3. Error ratio of method 1, $\lambda = 0.638\,\mu m$ (from ref. 8)

## 2.2 Description of Instrument

An instrument, based on the above approach and consisting of four main parts, namely, the He-Ne laser, an optical system, an electronic control system, and an output recorder, has been built and tested. A schematic layout is shown in Fig. 5. Pictures of the device is shown in Fig. 6 and 7. The reader is referd to Ref. 1 for more information about the rearanged device.

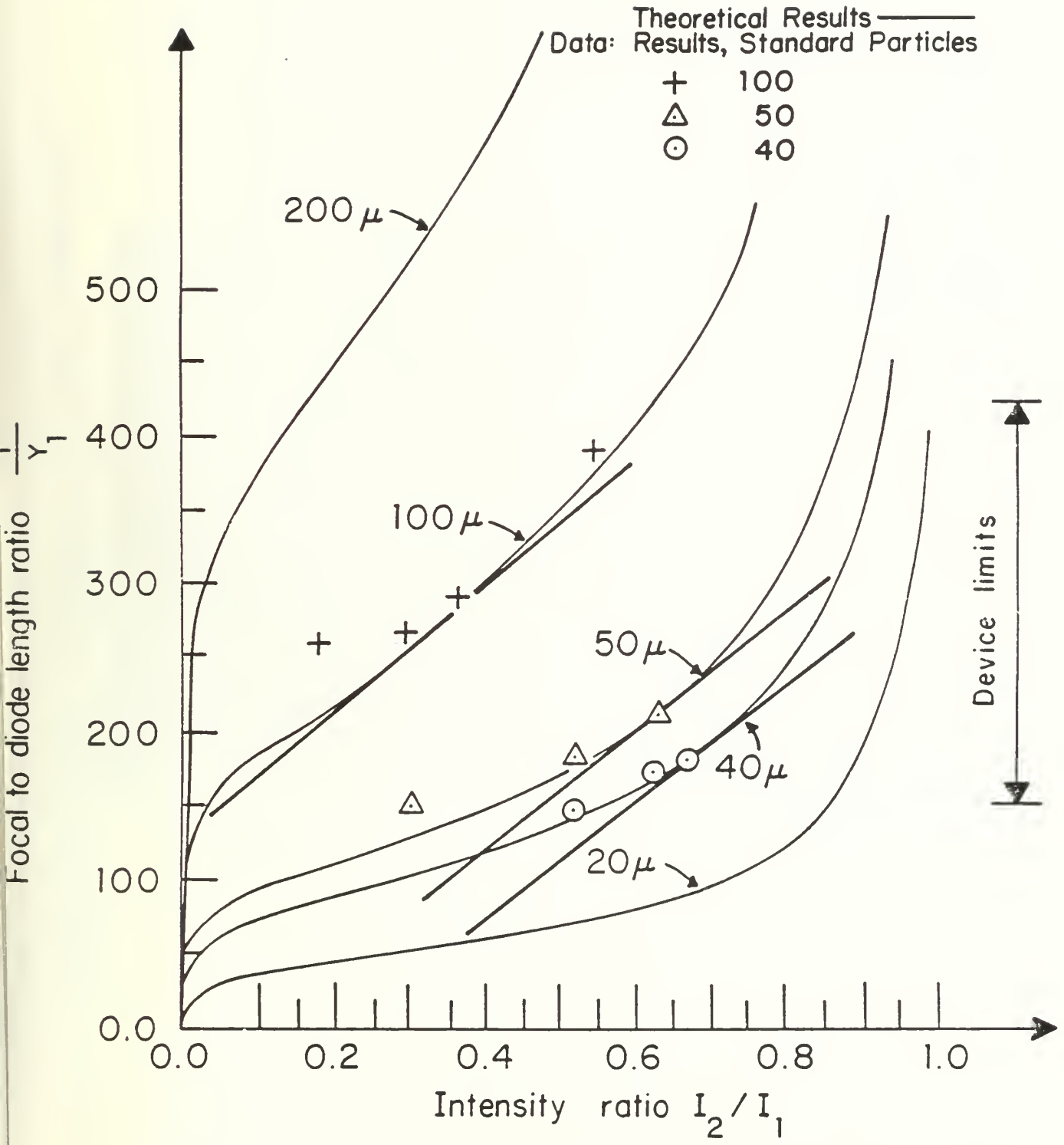


Figure 4. Comparison between Theory and Measurements, Variable Focal length control with various intensity ratios.

$$\left(\lambda = 0.6328\,\mu m,\ \frac{\theta_2}{\theta_1} = \sqrt{2}\right)$$

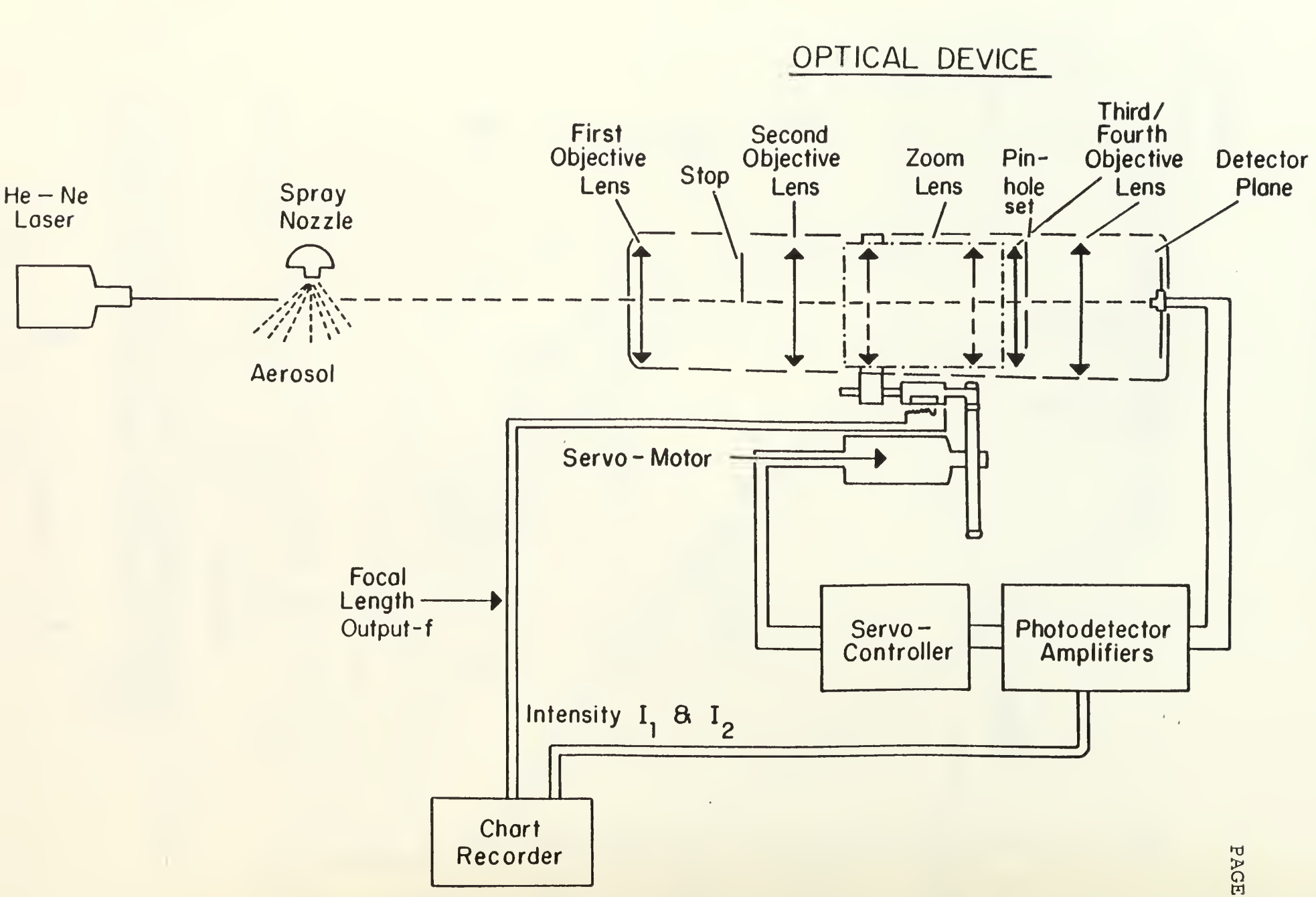


Figure 5. Schematic diagram of Optical Experiment Apparatus.

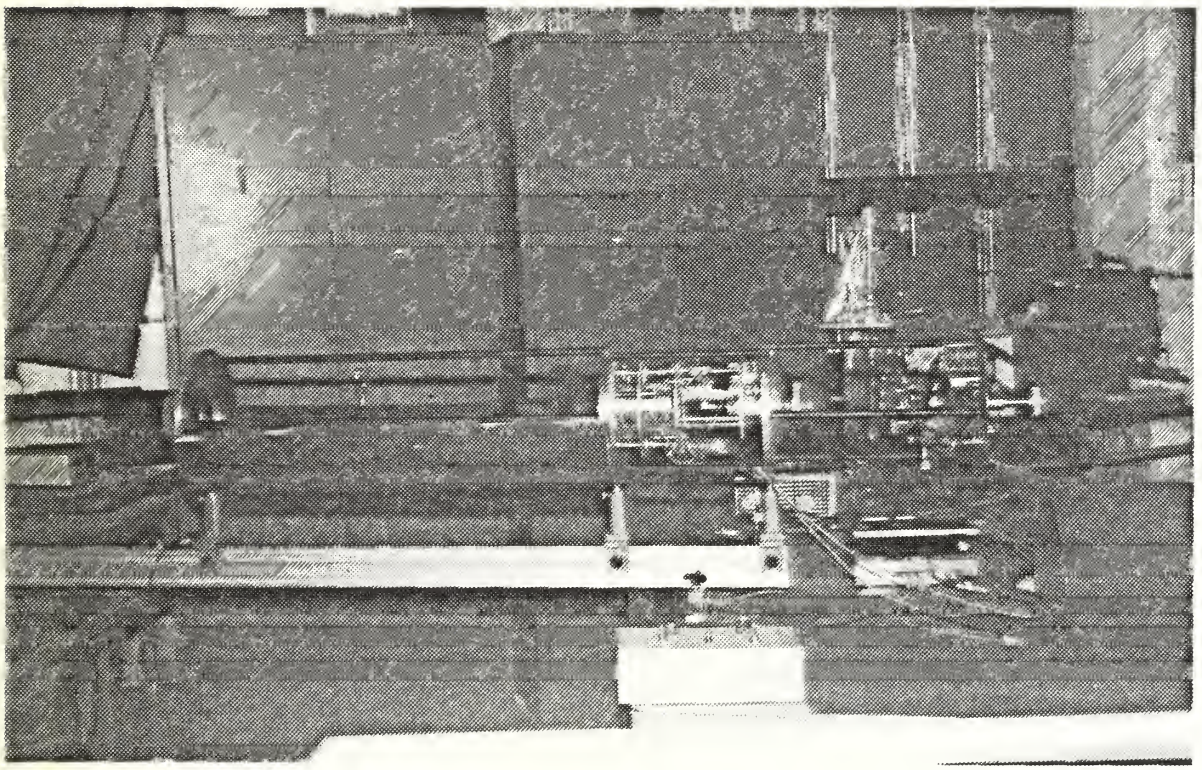

Figure 6. OPTICAL APPARATUS- WITHOUT TUBE COVER

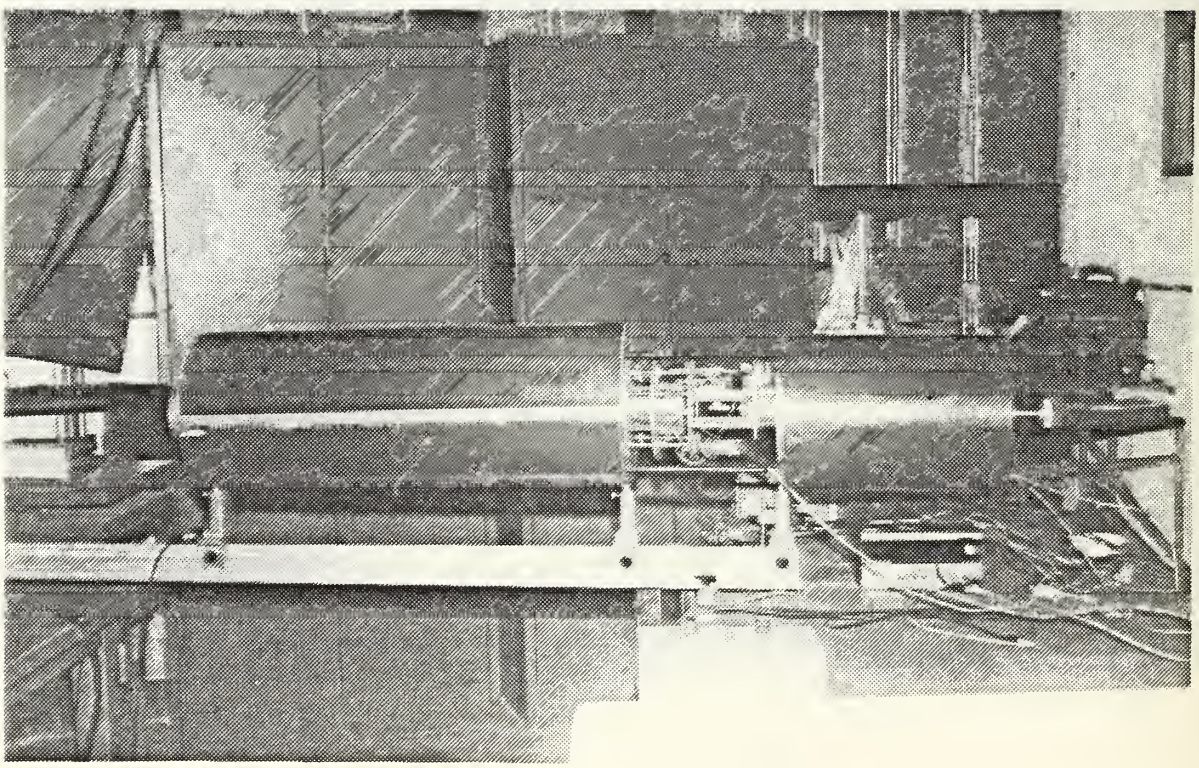

Figure 7. OPTICAL APPARATUS - WITH COVER

## 2.3 Calibration and Operation

The procedure for calibration and operation the system consists of: Alignment and calibration of the optical system, calibration of the gain voltage of the two photodetector channels with respect to intensity ratio, and calibration of the entire system using various sized standard aerosol particles. The initial focusing and calibration of the optical system is greatly facilitated by the use of a precision collimator.

Once the various optical elements had been correctly aligned and brought into focus with collimated light, a precision collimator was used to calibrate the overall focal length of the objective as a function of the position of the focal length setting micrometer screw. Gains of the signal conditioning amplifiers were adjusted to various intensity ratios using a small laser as a light source and a calibrated optical attenuator.

From Fig.4 we see that for the range of focal lengths available with the present instrument, that particle sizes from at least 40 to 100 microns should be readily detectable. Moreover, each of those particles may be detected over a practical range of intensity ratios. In order to select optimal intensity ratios for the detection of each particle size, a resolution parameter is defined as the change in focal length necessary to provide a unit change in intensity ratio. Using Eq. 7 we obtain:

$$(8) \quad R \equiv \partial(f/y_1)/\partial(I_2/I_1) = \sqrt{2}\, D_{32}[(I_2/I_1)\ell n(-I_2/I_1)]^{-3/2}$$

The normalized resolution, $R/D_{32}$ , is plotted in Fig. 8, and is seen to have a minimum at $I_2/I_1$ =0.223. For values of intensity ratio less than this minimum, the servo control system becomes unstable and the satisfactory operation of the instrument dictates that actual intensity ratios be greater than this minimum. The upper limit in intensity ratio which may be employed, given the limits imposed by the focal length range, is seen to be particle size dependent in Fig. 4. Selection of intensity ratios is constrained by these considerations and values above 0.4 and below the upper limit are preferred in order to minimize sensitivity.

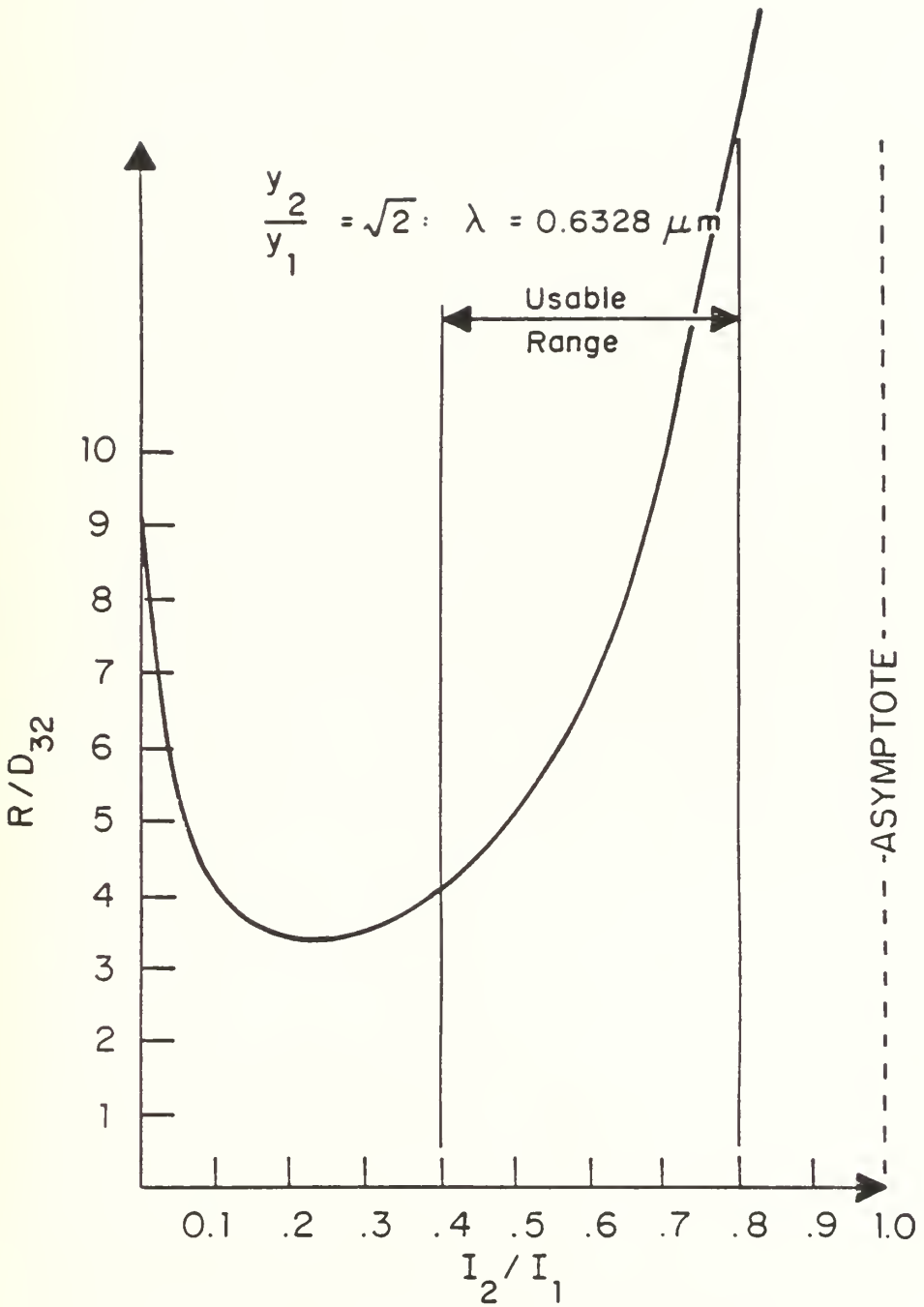


Figure 8. Normalized resolution value distribution as a function of intensity ratio.

Actual calibration of the instrument at several different intensity ratios was carried out using suspension of 40, 50 and 100 micron diameter standard particles in distilled water. Optical absorption of the distilled water and the walls of its glass confiner were nulled in the measuring system through adjustment of the offset of the signal conditioning amplifiers. The results of the calibration procedure are shown plotted in Fig. 4. It was found that a lower limit of useable intensity intensity ratio existed for each particle size which corresponds to the resolution limit of the optical system. This is, of course, a function of the quality of the various optical elements which constitute the entire optical path. For the system described here, the limit of the useable resolution was found to correspond to the value of the resolution parameter, R, in Eq. 8 of 400. This in turn corresponded to minimum useable intensity ratios, ( $I_2/I_1$ ), of 0.71, 0.66 and 0.4 for 40,50 and 100 micron aerosols.

2.4 Measurements

Once the system calibration and resolution limit, R, has been determined, Eq. 7 may be used to determine the Sauter Mean Diameter of an unknown aerosol. This was done using the fuel spray from a jet engine fuel injector nozzle as the source of aerosols. In the range of Sauter Mean Diameter of about 50 microns it was possible to resolve 0.1 microns. For example at an injection pressure of 125 psi it was found that the Sauter Mean Diameter of the aerosol spray produced was 51.7 microns corresponding to f=2775 mm and $I_2/I_1$ =0.67 when the injection pressure was reduced to 80 psi an aerosol spray having Sauter Mean Diameter of 47.8 microns corresponding to f=2614 mm and

$I_2/I_1$ =0.68.

2.5 Conclusions for the Cold Tests.

A technique for inferring Sauter Mean Diameters of aerosols using forward scattering of light, (Fraunhofer scattering), coupled with the assumption of a Gaussian distribution of particle sizes has been described. Introduction of an optical element of variable focal-length, (a zoom lens), permits a range of effective instrument focal lengths to be obtained and in turn broadens the range of particle sizes which may be detected by a single instrument, representing a substantial improvement over previous techniques based on fixed focal length optics. Actual measurements of fuel spray aerosols indicate the instrument is capable of measurement resolution of about one percent. Although no great attention was paid to the quality of the optical elements employed, a satisfactory optical resolution resulted. Optimization of the elements offers a further opportunity to broaden the usable range of the instrument.

## 3. PROPOSED IMPROVEMENTS FOR THE OPTICAL DEVICE

While working with the optical device some ideas for improvement arose. Let us look first at the main error sources, which are known to be:

A. Objective lens focusing.

B. Backlash on the gear transmision from the electric motor to the zoom lens.

C. Stability and stiffness of the device construction.

D. Photodiode main focal plain focusing.

In order to overcome these main error sources the following design improvements were made: The ability to move the objective lens, into a precise focusing spot is limited under the present conditions. As it is shown in Fig. 9, it is proposed to install the objective lens in a tube, and with the aid of a leading screw this will enable to slide the objective lens together with its tube along the axis, while the screw will move inside an helical splint in the outer cylinder. That will increase the traversing distance and align the objective lens.

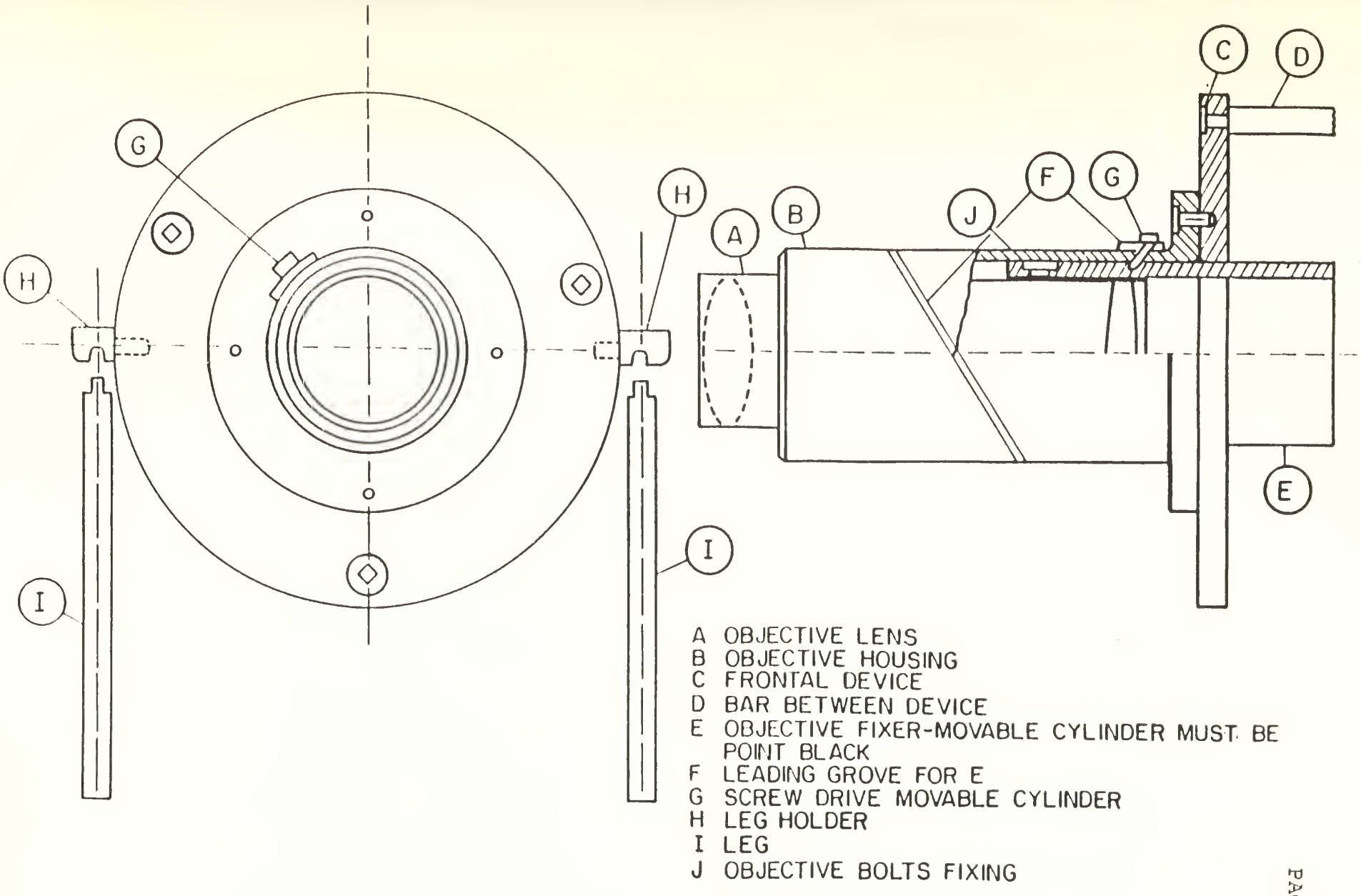


Figure 9. OBJECTIVE MOVABLE HOLDER AND DEVICE LEANING LEGS

In the present device, the traversal of the zoom lens is caused by a rotational electric motor through several teeth wheel. A better way to exert translation is by direct connection of the zoom lens to a linear step motor. This type of movement transmition will save difficulties in backlash problem and time response for the control loop. A step motor was purchased but has not been installed yet. This step motor would be installed directly behind the flange that holds the zoom lens. In Fig. 10 a general cross section is presented with all the improvements.

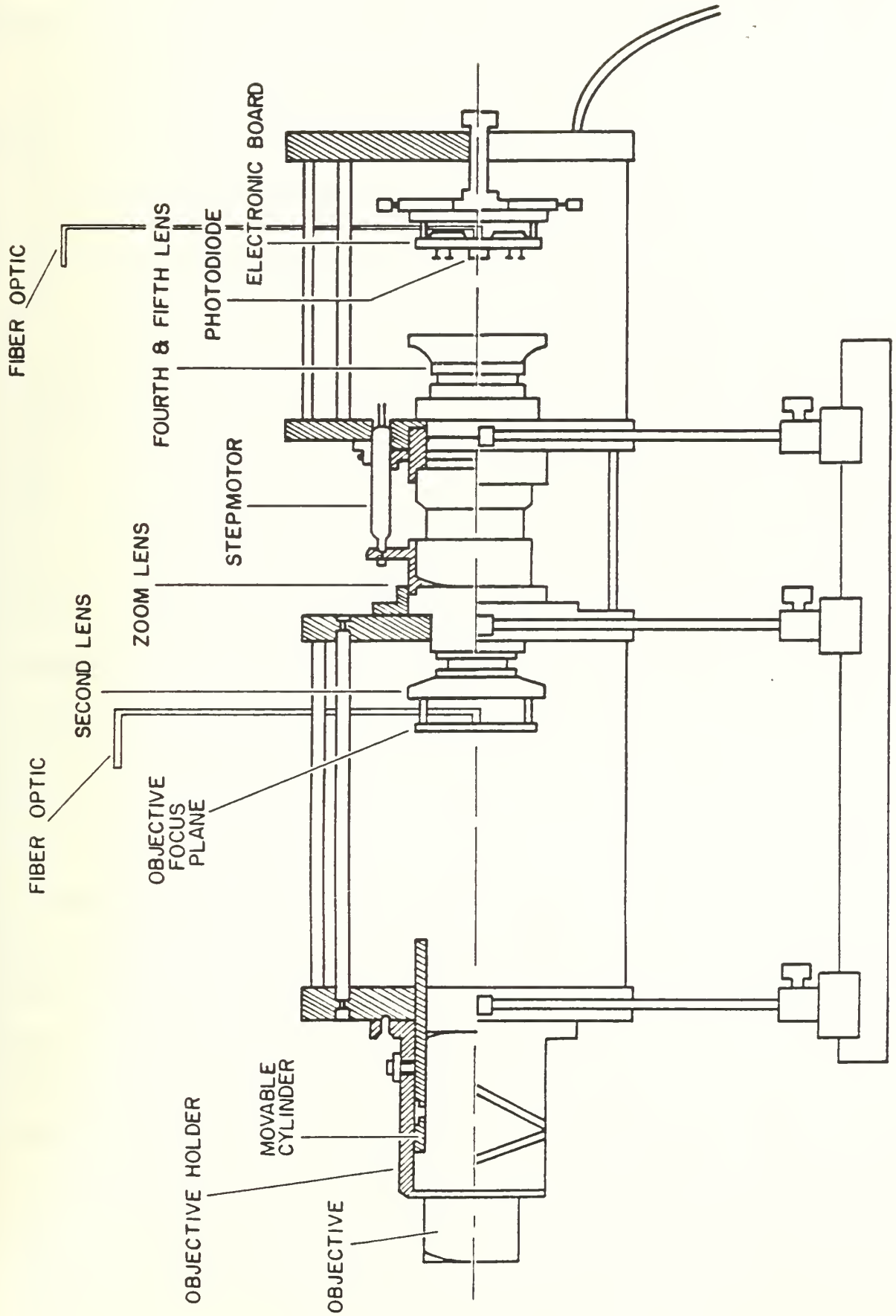


Figure 10. OPTIC DEVICE CROSS SECTION

The device is loaded in the in the perpendicular direction through three seperated legs, as shown in Fig. 9 and 10, each leg carrying part of the load along the focal axis. This kind of mounting does not prevent the device from vibrations in the plane which is perpendicular to the focal axis. In order to prevent this degree of freedom, it is recommended to mount the device on two legs at the sections where the single legs are located presently. The ears would be screwed in, in each mounting case flange, in the two sides of it, each ear has a screw hole for its leg. The left and the right legs will be fastened to triangular sliding bars, by standard leg holders, as shown in Fig. 9. This kind of mounting will solve the problem of stiffness of the device.

The procedure for alignment and focusing is a difficult job for one operator. In order to simplify this task it is recomended to work with two fiber optics strands. One would be located in the objective focal point and the other in the focal point of the photodiode plane. The two fiber optic strands would be carried out of the device toward the position of the laser source light aiming; this would enable the operators to aim the light rays exactly to the objective focal point , as the first step of alignment. The second step would consist of focusing by sliding the objective to get a sharp focal point in its focal plane, then the fiber, located at the focal point, would be removed, and by sliding the diode plane in the x-y and z directions, one would be able to locate the focal point in the entrance of the second fiber. As this fiber would be located exactly in the origin of the photodiode x-y axes, and the photodiodes are fixed to the same plane of the fiber entrance, photodiode distances would be certain and

the device would be aligned.

All the above improvements are mechanical in nature and address directly the main error sources in the present apparatus. There are two other types of improvements to simplify the electronics part of the device. One concerns the amplifier channel circuit and its circuit board and the other concerns to the type of calibration of the total gain-ratio. The previous electronic circuit was built just with the internal builtin diode without using its inernal, also builtin, amplifier. Each channel signal was amplified through three different output circuits stages. The two channel amplified signals are subtracted and the subtraction signal provides the input for the servo-control circuit. All that electronic circuits were built on one elecronic board which is located inside the apparatus; this kind of arrangement caused difficulty sometimes when approaching the gain resistor for gain adjustment purposes. Checking one photodiode with its internal amplifier revealed that with a 1MΩ gain resistor an high level output, of 2.5 V with low noise level can be achieved, for a 1mW laser light source. Therefore the electronic circuit was divided into two parts. The first part is an electronic board consist of four photodiodes (two pairs) with its gain resistors, this board is placed in the x-y focal diode plane. The other part is also an electronic board contain all the rest stage amplifiers, offset resistors, substractor and its amplified signal. This board is located outside the apparatus and makes the adjusting , during calibration procedure much simplier. Unfortunatly most of the internal photodiode's amplifier were found out of order, therefore it its highly recommended to check each photodiode before installing it into the circuit board

The other improvement concerns with the calibration procedure, is to simplify it by switching the output of a photodiode to either gain channel and measuring the output each time, the division of the two output measurement, $V_i^1/V_i^2$, is the total gain ratio of the two channels. If $V_i^j$ indicates the measured amplified output signal of diode i through channel j, and $a_j$ is the channel gain, then one can write:

$$V_i^1=a_1 I_i \quad \text{and} \quad V_i^2=a_2 I_i$$

Therefore the gain ratio of the two channels is directly proprotional to thier output voltage ratio:

$$a_1/a_2=V_i^1/V_i^2$$

This can be checked for several intensities $I_i$ in order to find the deviation and uncertainty of the two channel gain ratio $a_1/a_2$. This is an improvement over the previous method for which a mirror travers the same source light from one photodiode to the other, a procedure which took a long time. The proposed method does not demands using the same light source for the two phodiodes, switching the gain channels to each diode simulate the same procedure, and therefore it can be done even during the test measurement.

## 4. CHANGING POLES IN THE HIGH VOLTAGE FUEL NOZZLE

Previous work, Ref. 2 done on the same subject of improving burning efficiency by means of high voltage electric field revealed the uncetainty to be overcome. One of its main recommendation was to replace its electrode, pointed against the fuel nozzle exit, by a plane electrode, called "Fly-Swater", and to charge the fuel before

spraying it, which meant to exchange electric field direction.

Three different parts were built in order to provide the same preformance of the fuel spray with its new positive high voltage connection. The fuel spray metal-mounting-base was replaced to a plexiglass material in the cold test, and phenolic material for hot tests purposes. The Fly-Swater for the cold tests, was made of a steel frame and 1 mm. copper rodes inserted into the circumefernce to provide a plane of zero potential againstthe high voltage fuel spray exit. (See Fig. 12) A frame made of tungsten rods made of platinum was built for the hot test Fly-Swater.

In order to prevent sparking between the charged spray nozzle and combustor nozzle intake, where the spray nozzle is mounted, it was indispensable to insert a dielectric material between the two parts without changing the free space for air entering the combustor chamber. Two ways were found to do that, one was to machine the intake nozzle of the combustor and to insert a thin dielectric cone into it; the other idea was to built a new nozzle cap made of an insulated material for the spray nozzle; in this case we had to be very carefull of not changing the dimensions of the exit spray nozzle holes. For reason of simplicity, and just for the model tests we prefered to change the spray nozzle cap, (Fig.11). In order to do that, we cut out an outlet face, which includes the holes, of an existing spray nozzle, then we reduced its outside diameter, without touching the holes. This modified original part was afterward inserted into a new teflon sleeve, with the proper outsides dimensions, and together they provided the insulated cap. A picture of it can be seen in Fig. 12.

A. TEFLON SLEEVE ADJUSTMENT
B. NOZZLE EXISTING OUTLET HOLES (STEEL)

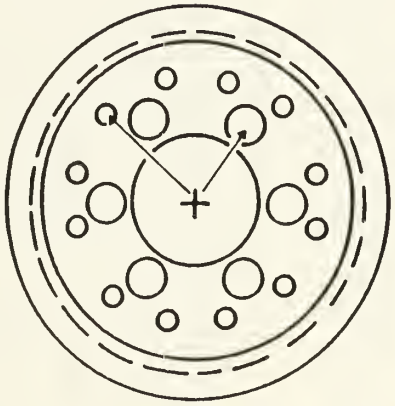

PART B

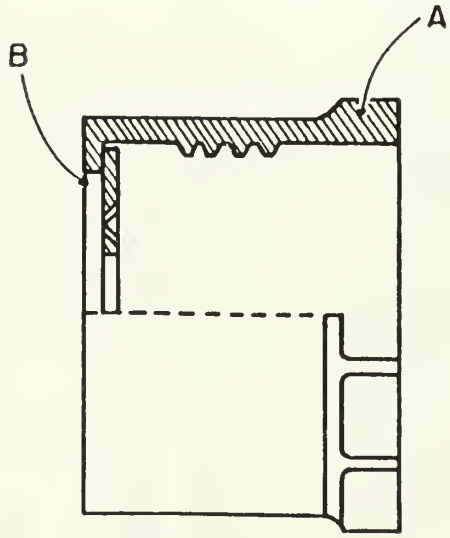


Figure 11. SPRAY NOZZLE HEAD INSULATION

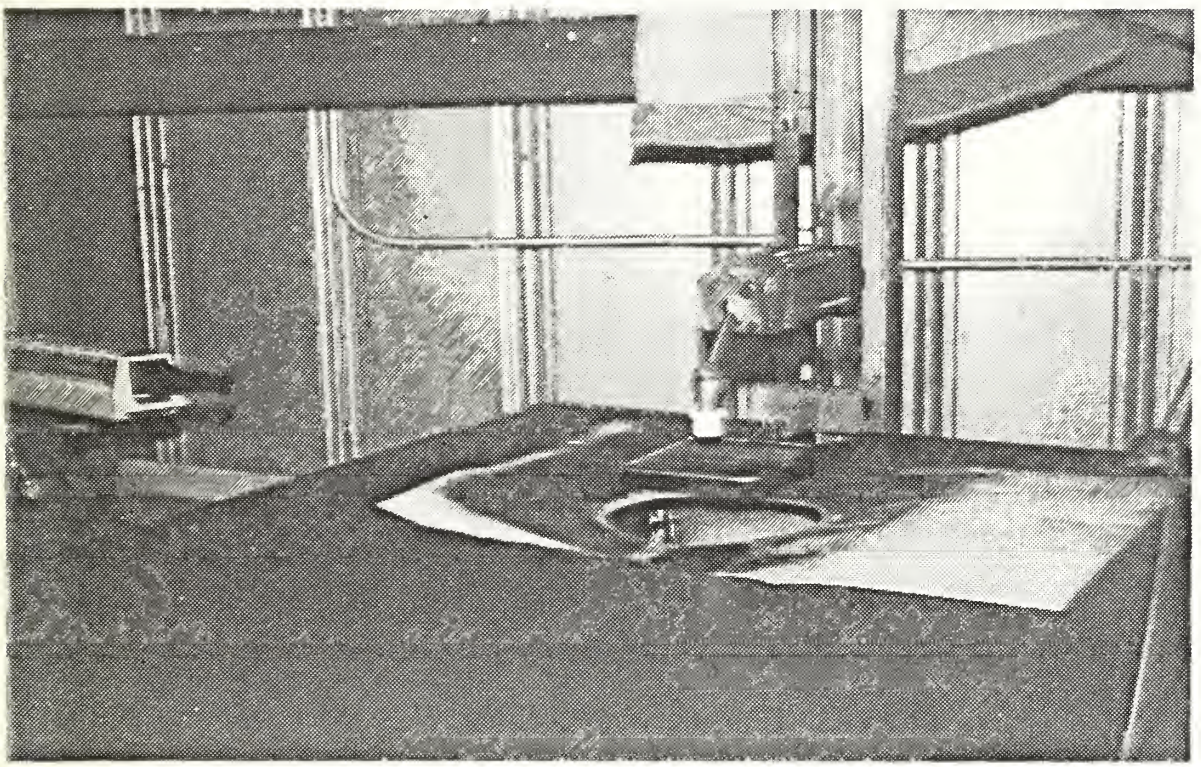

Figure 12. FLY-SWATER and TEFLON CAP in COLD TEST ARRANGEMENT

After mounting the teflon cap, the fuel spray was tested with the optic apparatus,up to 150 psia fuel pressure, and found to have the same SMD as the original fuel spray nozzle. This fact assures the same preformance to the insulated fuel spray nozzle. Testings with an opposed electric field, with the of the aid of the Fly-Swater were also done. The Fly-Swatter was 4.5 mm. apart of the nozzle exit, the voltage exerted up to 24 KV and the optic measurements taken of the fuel jet between the nozzle exit and the Fly-Swater did not show a change in the SMD, at least the optical apparatus could not resolve any change during these preliminary tests.

Two other phenomena were easily observed, while exerting the high voltage field: A change in the spray cone angle and a significant change in a single droplet size which cross the distance from the nozzle exit to the Fly-swatter, by a free fall motion. The first observation was also reported and measured in Ref.11. The observed change in the diameter size for a low speed droplet, and an unchanged mean droplet size as measured in the cold fuel spray, with relatively high droplets velocities, can be explained by one of the following reasons: According to REf. 12, as the relative droplet to air velocity increases the electric field influence effect decreases. However, using the empirical nondimensional equation provided by that Ref. 12, one can find a maximum relative droplet change in diameter is 18 precent. But in our system, it may not be seen because of high fluid velocities, which may prevent droplets of having been charged. Also mentioned by the above reference that for droplet velocities higher then 30 meter per second with high voltage field change in SMD may fall below 4 percent, which is under the limit of an optic apparatus

such as ours based on the the Gasussian approximation.

## 5. HOT TESTS

The objective of the hot tests was to find out whether there is any change in the flame temperature while exerting an high voltage electric field, during a regular performance of the T-56 jet combustor. The difference between those test to those done in the previous work, Ref.2, is in running the test under a better simulated environment of pressure, and checking the new consideration for opposite poles under those conditions.

### 5.1 Preparations.

In order to have a better simulation of the jet combustor performance in the combustion laboratory simulator device, we had to maintain an outlet pressure of the range of 1.5 to 2 atmospheres. Previous outlet pressure was atmospheric. Along with the outlet pressure simulation demands, mass rate flow and combustor total temperature must also be in expected given range. From Ref. 2 we found that the range for the mass flow rate must be between 2500 lbm/hr to 3483 lbm/hr and the temperature range should be from 1787°R to 2460°R. A pressure chamber, connected to the outlet of the combustor chamber, together with two different choked nozzle were designed and built to preform in the above preformance envelop.

With the aid of the equation of a nozzle choked flow, using the the thermochemical program results for that combustor of average heat capacity ratio of 1.3 and assuming a friction coefficient of 0.98, we came up with two sizes of throat nozzles, one with a 1.68 inch throat

diameter and second one of 2.11 inch. Each flow nozzle covers an other region of mass flow rate (in lbm/hr) as a function of total pressure $P_0$ and static temperature, T.

Preformance of each nozzle, in units of mass flow rate, is given below:

| | $D^*$=1.68 inch | | $D^*$=2.11 inch | |
|---|---|---|---|---|
| $P_0$ \ T(°R) | 1787 | 2460 | 1787 | 2460 |
| 22. Psia. | 2180 | 1858 | 3458 | 2947.5 |
| 29.4 Psia. | 2907 | 2478 | 4612 | 3931 |

The design of the two nozzles is presented in Fig.13. They were installed at the end of the pressure chamber, which its design is presented in Fig. 14. On the left hand side of the pressure chamber we welded a flange to connect it to the combustor chamber by twelve existing bolts, on its other side the pressure chamber has an outlet flange with a special hole for screwing in one of throat nozzle described above. The pressure chamber has two side holes, one for the thermocouple-wires and the other for a pressure tap. There were four thermocouple-wires connected to the combustor outlet, three of them were made from chromel-alumel (Omega type K), they were inserted inside a ceramic radiation shield. Two of them were placed in each side of the combustor outlet and third one in the center. The fourth thermocouple was made from Pt-Pt/Rd(3%) (type R) and was installed together with one of the side thermocouples. The three type K thermocouples were connected separatly to a chart recorder, while the platinum went through a special amplifier and display to the chart recorder.

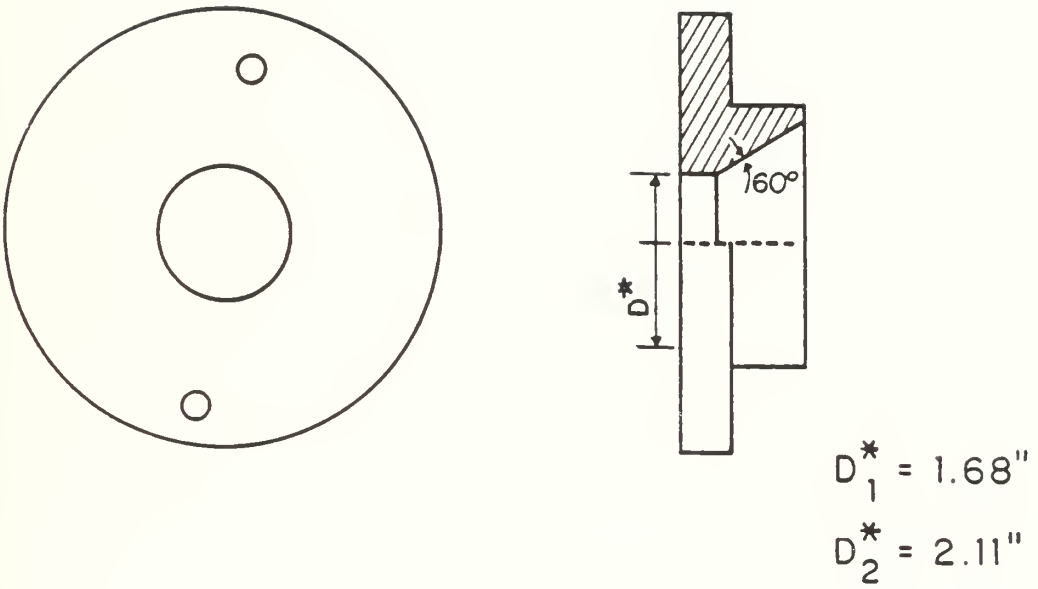


Figure 13. PRESSURE CHAMBER NOZZLE

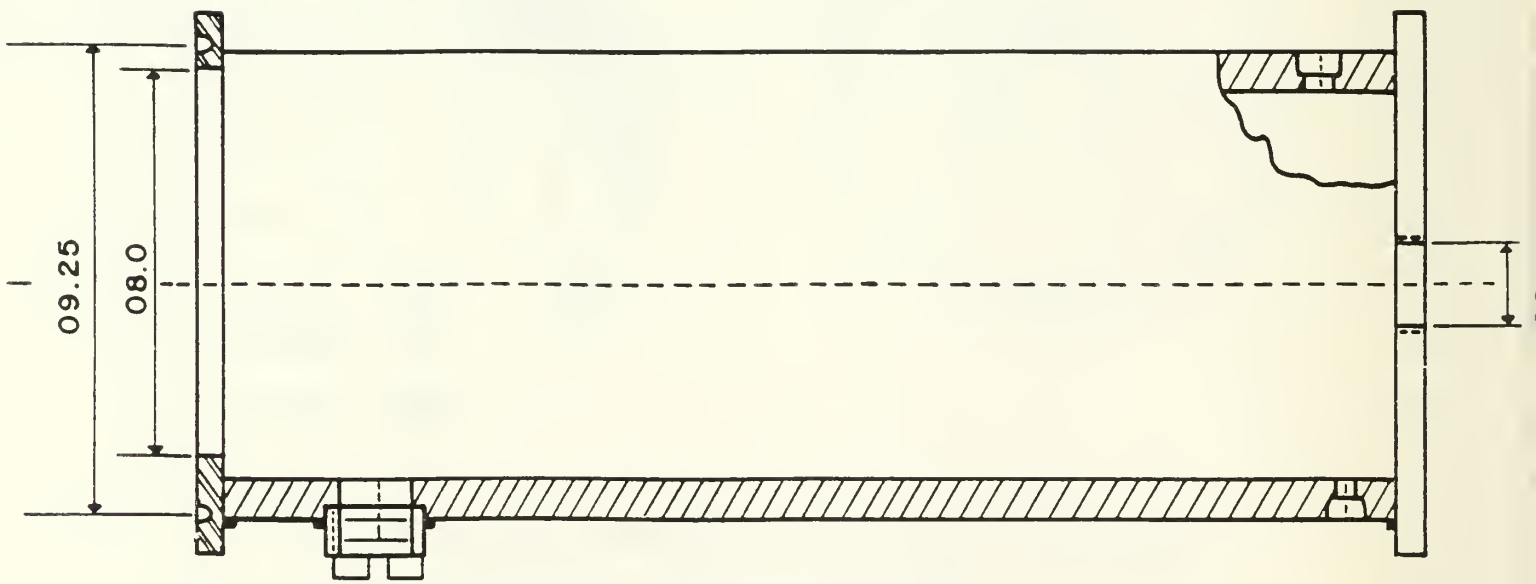


Figure 14. PRESSURE CHAMBER

In Fig.15 we present a picture of the assembled parts. The fuel was supplied from a 3-liter pressure vessel through a Turbine Flow Meter (TFM). The fuel mass flow rate was calibrated against various pressures vessel whereupon any pressure defines a mass flow rate and a specific output voltage from the TFM. The thermocouple chart recorder was also calibrated with an aid of a standard millivolt power supply. We used the calibration chart for the air supply given in Ref. 11. The pressure on the chamber pressure was measured by a simple visual gage. The fuel rate flow and the air rate flow was recorded on a different chart recorder. A schematic arrangement of the measurement and combustion device is shown in Fig.16. The high voltage power supply provided the voltage for the electrode, and its output was recorded on the thermocouples chart recorder. We used the high voltage electrode with purged nitrogen, described in Ref. 2. The precise location of electrode's edge, inside the combustor was determined with the aid of a periscope fiber optic unit which includes a connection to an outer light source. After completion of the above preparation the device was ready to measure the parameters needed to indicate change in the combustor efficiency with an high voltage electrode and higher outlet pressure. The next planned step was to use the grounded Fly-Swater electrode and to find out if there is any difference in the combustion preformance while changing electrode poles. But unfortunatly this step could not be achieved because the fuel spray nozzle base, which was made of a phenolic material, became chared and shorted charged fuel nozzle.

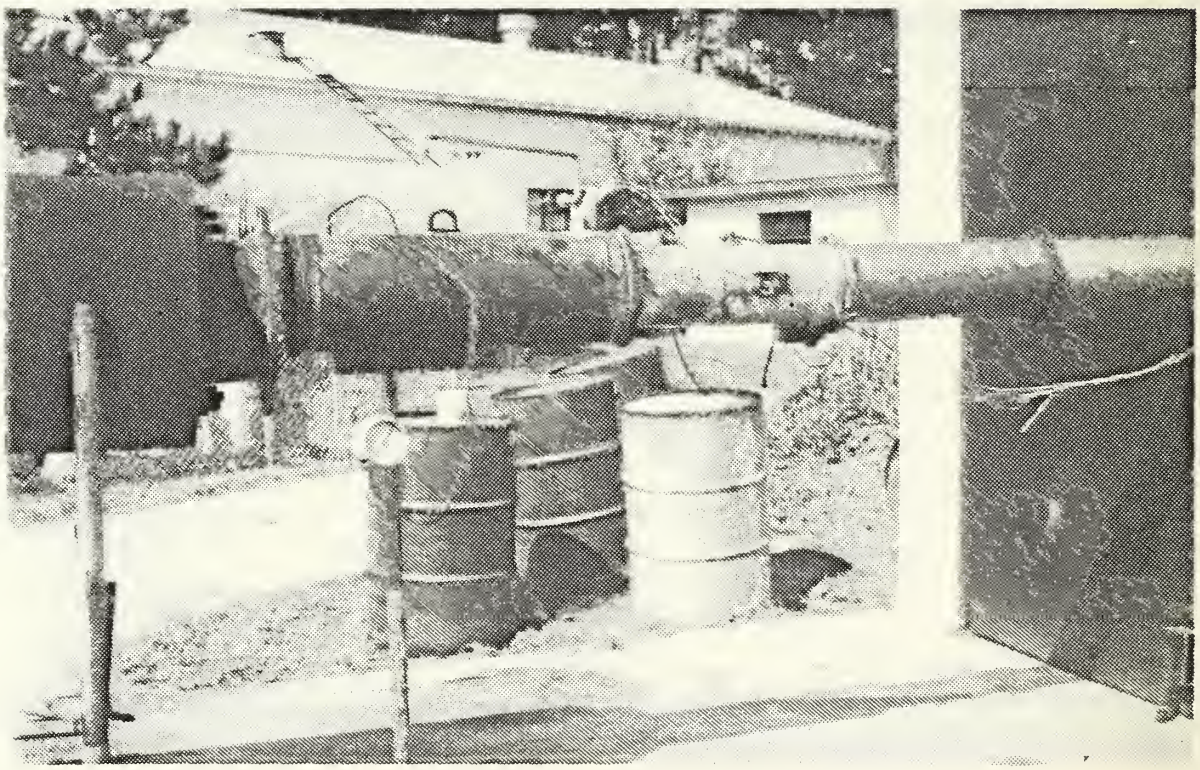

Figure 15. COMBUSTION and PRESSURE CHAMBERS

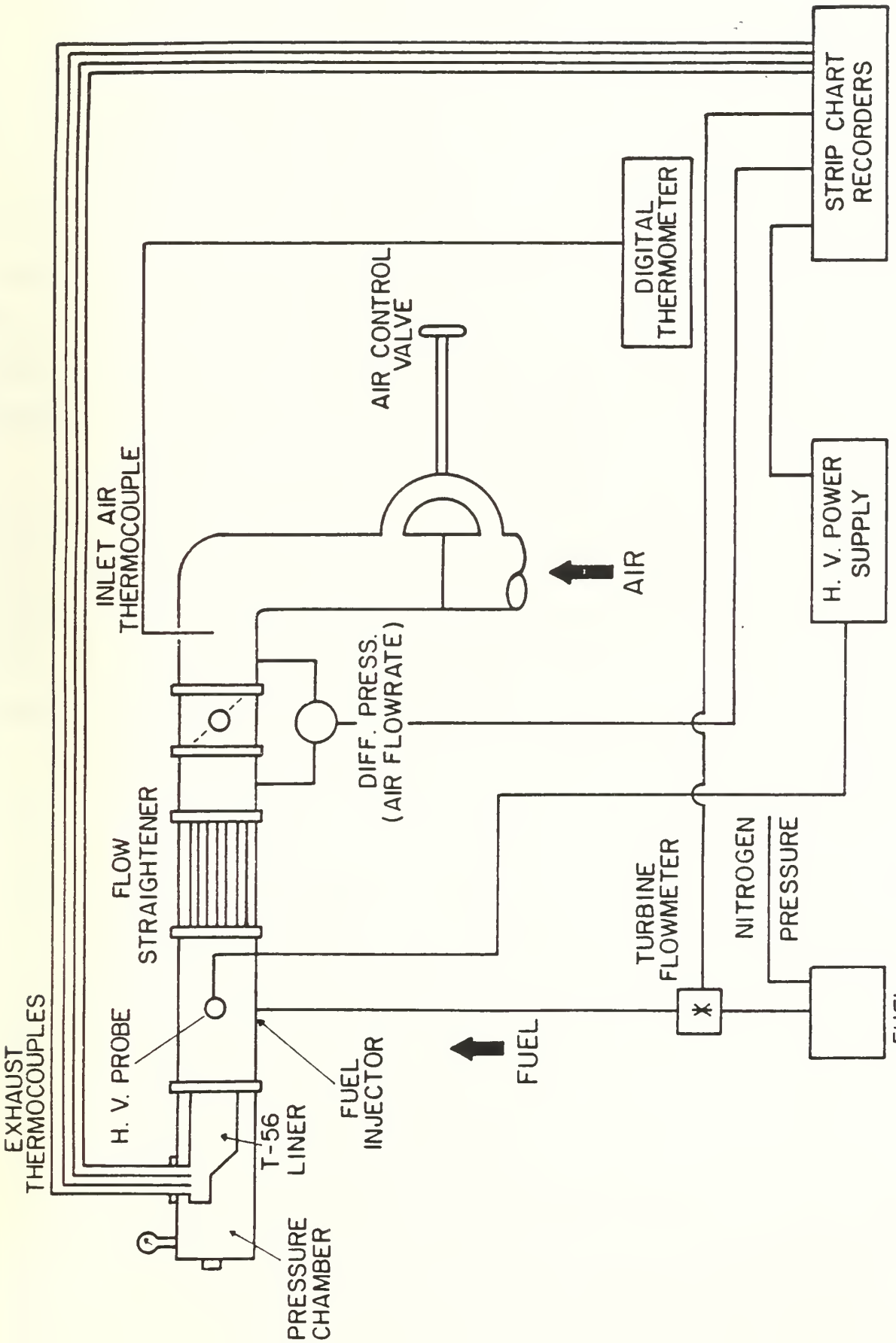


Figure 16. SCHEMATIC DIAGRAM OF THE COMBUSTION APPARATUS

5.2 Hot Test Measurements

Tests were carried out with Diesel (DF-2) fuel, with the above mentioned device. Each test began with an ignition procedure, of low air mass flow, and constant fuel mass flow, after ignition the air flow rate is increased manually and then the measured temperature and pressure becomes stabilized, at that time the high voltage is switch on. In Table 1 we present the result for the combustor test, and Fig.17 shows a typical chart recorder output of temperatures and voltage during the firing time. Those results indicate the following conclusions:

-Compressor air supply is not sufficient to maintain the demand for air mass flow together with higher outlet pressure greater than 14.5 psig, even with the smaller nozzle 1.68 inch. When the combustor ignites the inlet air pressure drops. preliminary tests with the greater nozzle (2.11 inch) showed insufficient pressure in the chamber pressure (not more than 5 psig).

-Temperature measurements on the combustor outlet cross section are very sensitive to their location, along the cross section and type of radiation heat shield. The type-R thermocouple which was inserted inside an indium radiation shield with a special hole for hot gas traveling through it, provided a much more stabilized temperature reading then the were overall shielded without any gas-junction contuct. Together with its amplifier, the Pt-Pt/Rd thermocouple shows a reliable stable output, and temperature pretubations according to change in the electric field could be recorded. Therefore just after the flame temperature was stabilized the high voltage was switch on. The pointed electrode which was as close as possible to the the fuel

spray exit , 7 mm apart, exerted a high electric field. But none of the temperature recorded had shown a change in the measured temperature.

-Soot was depositing on the pointed electrode, after several combustor operations, and caused an electric short.

-During some failure of ignition, fuel the insulation base of the spray nozzle , which caused its burning immediatly after the first ignition and back-fire. As a consequence the phenolic material became charred.

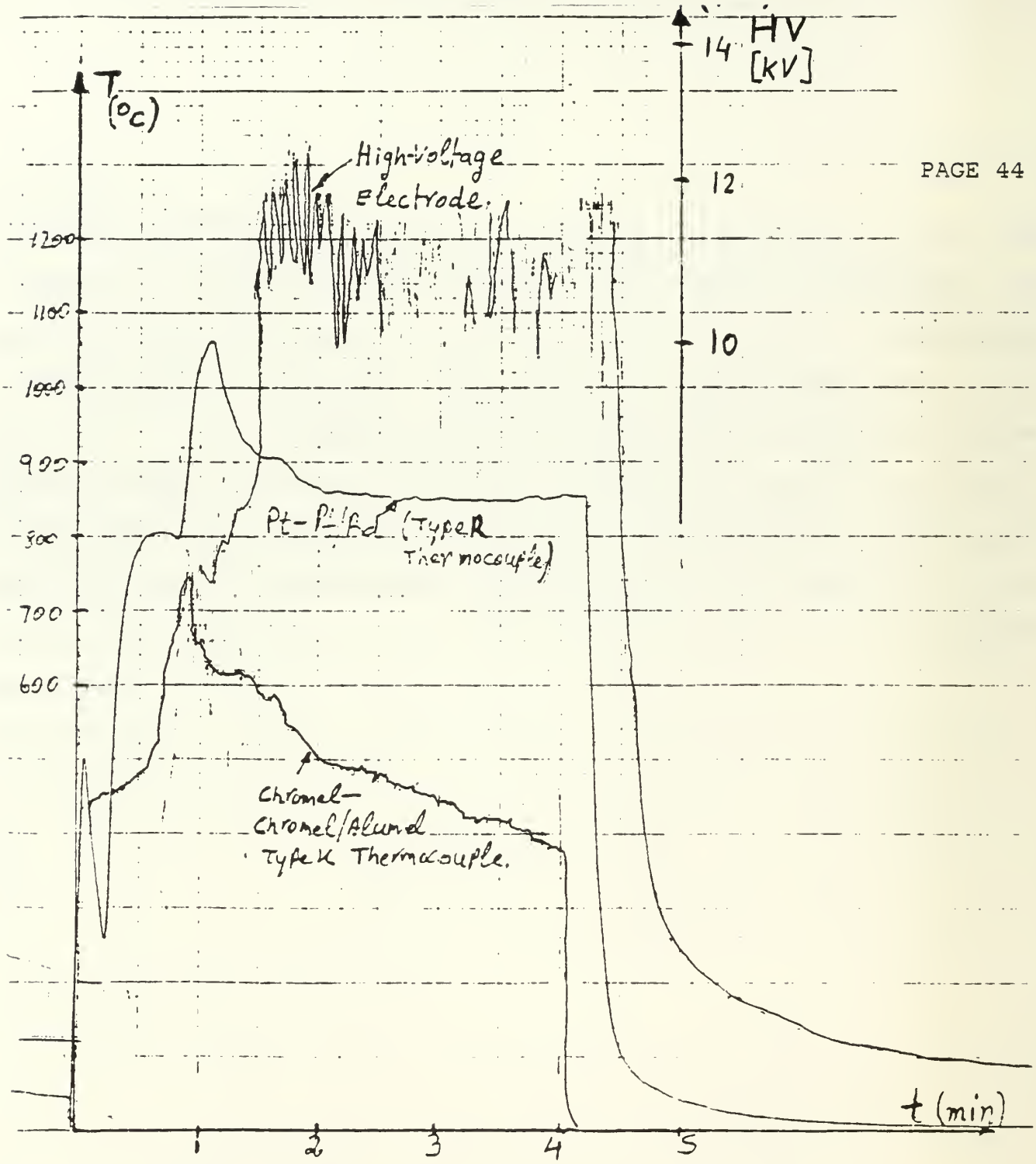


Figure 17. TEMPERATURE-VOLTAGE DISTRIBUTION WITH TIME

Table 1: Hot Tests Results

$D^*$ = 1.68 inch Fuel: DF-2

r = 0.06809

| $m_a$ | $m_f$ | T | ER | P | V | Remarks |
|---|---|---|---|---|---|---|
| lbm/hr | lbm/hr | °c | | psig | KV | |
| 2000. | 85.74 | 1342. | 0.629 | 14.5 | 0. | |
| 2854 | 84. | 1200. | 0.432 | 12. | 0. | |
| 1583. | 67. | 943. | 0.62 | 13.5 | 0. | |
| 2083. | 87. | 1310. | 0.613 | 14.2 | 0. | |
| 950. | 77. | 580. | | 5. | 0. | |
| 2500. | 68. | 885. | 0.399 | 13. | 12-16 | No Change |
| 2520. | 85. | 1110. | 0.495 | 14. | 10-12 | in Temperature |
| 3500. | 76.3 | 600. | 0.32 | 10. | 4,12,20 | Recorded |

5.3 Hot Tests Improvements

As a result of using the combustor with a pressure chamber new difficulties arised. Other parts such as the electrode and the insulated nozzle spray base also caused problems and needs some improvements. We would also like to mention that there is was lack of a precise digital device which could scan for the measured parameter in real time. Without such a device results are difficult to interpreted.

In order to maintain constant flow with high pressure combustor outlet, as to simulate the combustor operation, there is a need to choke the flow before its entering to the combustor, this demand needs a much higher air mass flow, which the present compressor can not provide. The 3-liter fuel vessel is a time operation constrain, it is recommended to use an original fuel pump that fits the preformance of combustor liner, that will enable a continuous time operation which is very much needed for jet combustion tests. In order to prevent electrical shortage of the fuel spray nozzle base, it is recommended to built it of two different metal blocks, which will be connected between themselves by a ceramic block, as shown in FIg. 18, good ventilation of the coming air will prevent soot deposition on the ceramics insulator. A better enterance location is recommended for the pointed electrod in order to prevent its soot coverage. In Fig. 19 a new location and a new type of electrode is presented. According to that concept the electrode enterance is on the inclined base of the combustor ,at the place where its edge is as close as possible to the fuel spray nozzle outlet and still does not spark with the highest

voltage, such a displacement is of the order of 5 mm.

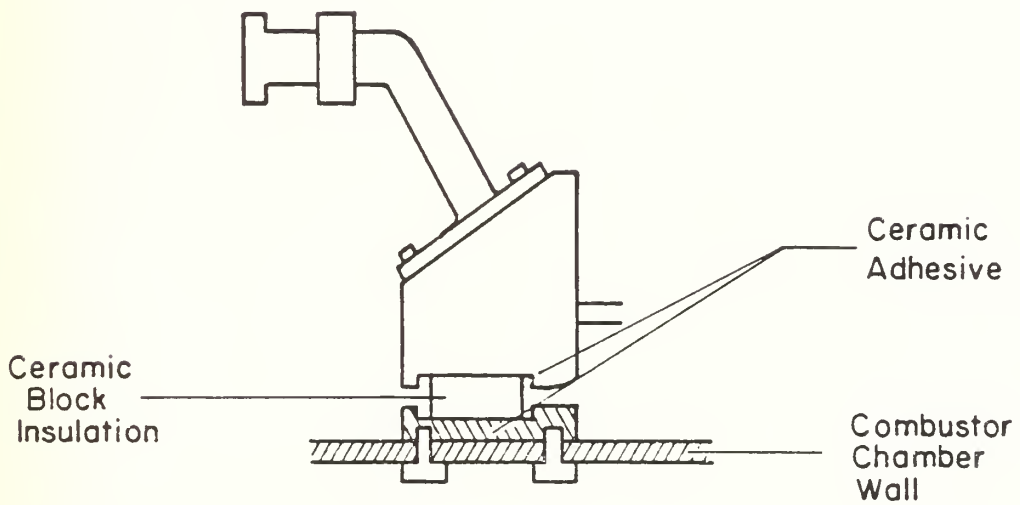


Figure 18. INSULATING THE FUEL SPRAY NOZZLE MOUNTING

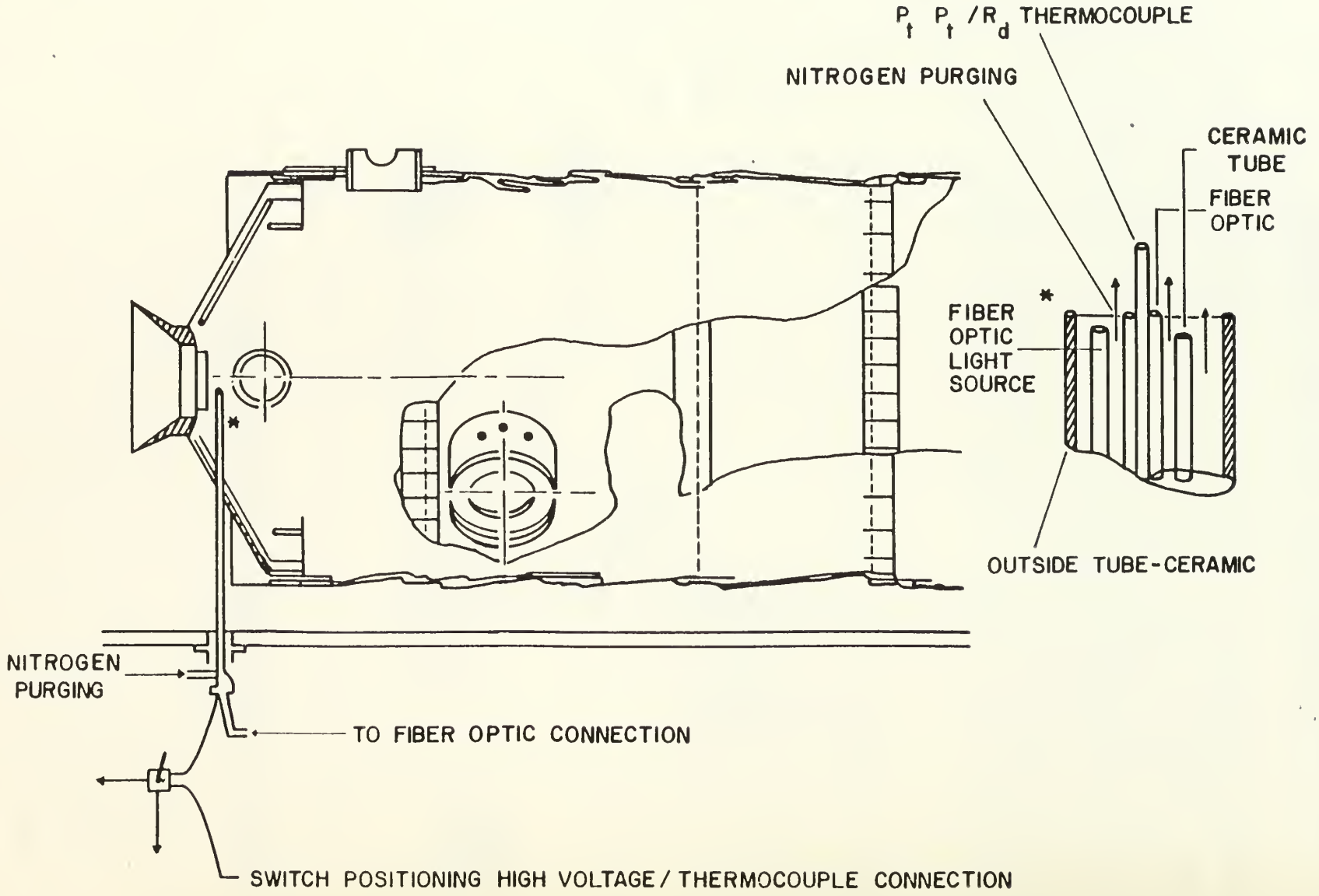


Figure 19. MULTIPURPOSE PROBE PRELIMINARY DESIGN

The probe insert would contain the following parts:

-Outer tube, shell protection.

-Two fiber optic, one which carry light to illuminate the edge electrode end the other to look at the electrode edge region.

-At the center of the shell tube there will be a Thermocouple/Electrode (TCE) made of platinum- platinum/ Rodium thermocouple. That can be used, by a special outer switching, as an high voltage electrode or a thermocouple. In order to prevent soot deposition and protect the fiber optics elements nitrogen should be purged inside the shell tube. With the aid of such a multipurpose probe it will be easy to measure the precise electrode location, temperature and temperature changes. By connecting the fiber optic edge to a magnified device and recording on a videotape one will be able to look at a droplet size change along its track and repulsion between the droplet inside the combustor.

# 6. CONCLUSIONS

An optical radiometer with variable focal length was developed and applied for measuring SMD changes in a diesel fuel spray. The present optical device needs further improvents, which are described in the report. Results of the tests, with the new radiometer could not resolve any significant change in the SMD under the elecrostatic field. Many more tests will be required with special attention to paid to the improvements for the radiometer.

The hot tests with the pressure chamber indicated the existence of a better outlet pressure for the jet combustor. The design for an improved point electrode for the combustor chamber, which would prevent electric shorts and permit better sensitivty in measuring temperature changes, together a with closer view of the spray near the elecrtrode, has been presented. The Fly-Swater elecrode design could not be tested because the charring of the phenolic material, which was used to insulate the spray nozzle, caused it to short to the chamber's wall. An alternate design for ceramic instead of a phenolic is indicated performed. The author would like to recommend to continue the research with the proposed improvements in order to get more precise data, for better understing the phenomena of electrostsic's field effects on comparatively high velocities fuel droplets and its influence on combustion efficiency.

REFERENCES

1. Powers J., Shavit Z., Biblarz O. and Miller J.A., "Variable Focal Length Radiometer for Particle Sizing," The 11th ICIASF conference Stanford, CA. AUg., 1985. School, Montery CA., December 1984.

2. Zajdman A., "Electrical Spray Modification with Various Fuels in a T56 Combustor," Contractor Report, NPS-67-83-003CR, Naval Posgraduate School, Montery CA., December 1982.

3. Miller, J.A., et al, "The Effect of Electrostatic Spray Modification on Combustion in Gas Turbines," ASME Paper 84-GT-102, 1984.

4. Dobbins, R.A., et al, "Measurement of Mean Particle Sizes of Spray from Diffractively Scattered Light," AIAA J., Vol 1, 1882, 1963.

5. Van De Hulst, "Light Scattering by Small Particles." Dover Press, N.Y., 1981.

6. Hodkison, J.R, "Particle Sizing by Means of The Forward Scattering Lobe," Applied Optics, Vol. 5, No. 5, May 1966, PP. 839-844.

7. Buchele, D.R , "Scanning Radiometer for Measurement of Forward Scattered Light to Determine Mean Diameter of Spray Particle," NASA TMX- 3454, Nov 1976.

8. Buchele,D.R., "Particle Sizing by Measurement of Forward Scattered Light at Two Angles," NASA TP-2156, May 1983.

9. Chin, J.H., Sliepvich, C.M. and Tribus, M., "Determination of Particle Size Distributions in Polydisperse Systems by Means of Measurements of Angular Variation of Intensity of Scattered Light at Very Small Angles," J. Phys. Chem Ithaca 5, pp. 841, 1955.

10. Ruscello, L.v.and Hileman, E.D., "Determining Droplet Size Distributions of Sprays With a Photodiode Array," Paper $WWs/CI-81-49,

Proceedings Fall Meeting Western States Section The Combustion Institute, Oct. 19-20,1981.

11. Laib, R.J., "Design of an Apparatus for the Study of Eelectrohydrodynamic Control of Spray from Fuel Injectors in Gas Turbines," M.Sc Thesis, Naval Postgraduate School, Montery CA., December 1982.

12. Smith, I.K. and Garmedia, L.A., "The Effect of an Electrostatic Field and Air Stream on Water Spray Droplet Size," Tran. IchemE, Vol. 57, 1979.

13. Harrje, D.T. and Reardon, F.H., "Liquid Propellant Rocket Combustion Instability," NASA SP-194, 1972.

# INITIAL DISTRIBUTION LIST

| | | No. Copies |
|---|---|---|
| 1. | Defense Technical Information Center<br>Cameron Station<br>Alexandria, VA 22314 | 2 |
| 2. | Library, Code 0142<br>Naval Postgraduate School<br>Monterey, CA 93943-5100 | 2 |
| 3. | Department Chairman, Code 67<br>Department of Aeronautics<br>Naval Postgraduate School<br>Monterey, CA 93943-5200 | 1 |
| 4. | Associate Professor O. Biblarz, Code 67Bi<br>Department of Aeronautics<br>Naval Postgraduate School<br>Monterey, CA 93943-5100 | 7 |
| 5. | Associate Professor James A. Miller, Code 67Mo<br>Department of Aeronautics<br>Naval Postgraduate School<br>Monterey, CA 93943-5100 | 7 |
| 6. | Mr. Z. Shavit<br>Visiting Research Associate<br>Department of Aeronautics<br>Naval Postgraduate School<br>Monterey, CA 93943-5100 | 2 |
| 7. | Commanding Officer<br>Naval Air Systems Command<br>Attn: Mr. G. Derderian, Code AIR-330B<br>Attn: Mr. T. Momiyama, Code AIR-330<br>Washington, DC 20361 | 10<br><br><br>1 |
| 8. | Dr. Alan Roberts<br>Headquarters, Naval Material Command<br>Energy and Natural Resources Research and Development Officer<br>Navy Department<br>Washington, DC 20360 | 2 |
| 9. | Mr. C. D. B. Curry, Patent Counsel<br>Office of Naval Research<br>One Hillidie Plaza, Suite 601<br>San Francisco, CA 94102 | 2 |

10. Dr. A. J. Kelly — 1
Department of Mechanical and Aerospace Engineering
Princeton University
Princeton, NJ 08544

11. Mr. J. Yount — 1
SA-ALC-SF TLA
Aerospace Fuels Laboratory
Building 70, Area B
Wright Patterson AFB, OH 45433

12. Dr. R. S. Golladay — 1
Director, Research and Development
Technology Division
NASA Headquarters
Washington, DC 20546

13. Mr. J. S. Grobman — 1
Chief, Fuels Technology Branch
NASA Lewis Research Center
21000 Brookpark Road
Cleveland, OH 44135

14. Mr. C. L. Delaney — 1
Airforce Aero Propulsion Laboratory
Wright Patterson AFB, OH 45433

15. Mr. R. A. Rudey — 1
NASA Lewis Research Center
2100 Brookpark Road
Cleveland, OH 44135

16. Mr. N. F. Rekos — 1
Office of Aeronautics and Space Technology
NASA Headquarters
Washington, DC 20546

17. Research Administration — 1
Code 012
Naval Postgraduate School
Monterey, CA 93943